Stopping Power of Be, Al, Cu, Ag, Pt, and Au for 5–12-MeV Protons and Deuterons

H. H. ANDERSEN, C. C. HANKE, H. SØRENSEN, AND P. VAJDA
Physics Department, Atomic Energy Commission, Research Establishment Risö, Roskilde, Denmark
(Received 1 August 1966)

Recent measurements on stopping power of aluminum have been continued with the stopping materials Be, Cu, Ag, Pt, and Au. The method of measuring stopping powers utilizing a thermometric compensation technique working at liquid-helium temperature has been used. Results are obtained with a standard deviation of 0.3%, and agree with other published experimental results and with Bichsel's tabulated values within their stated errors.

I. INTRODUCTION

FOR many years measurements have been made of energy losses and ranges of protons and deuterons. The best accuracies previously obtained were 0.5% for range measurements,[1,2] between 1 and 2% for absolute stopping powers,[3] and 0.3% for relative stopping powers.[4,5] Bichsel[6–8] has recently tried to present a detailed comparison between available experimental data and theory. It turned out, however, that the accuracy of existing data was usually not high enough to yield unambiguous results for the free parameters in the theory, and there is thus a need for still more accurate data.

From an experimental point of view, too, accurate stopping power data are of interest, when energy losses suffered in foils, windows, counters, etc. have to be calculated. Especially for nuclear emulsion it is important to have good results which can be extrapolated to high energies with increased accuracy.

The relativistic Bethe formula (see e.g. Ref. 9) for the stopping power is

$$-\frac{dE}{dx}=\frac{4\pi e^4 z^2 N_0 Z}{mc^2\beta^2 A}\left[\ln\left(\frac{2mc^2\beta^2}{1-\beta^2}\right)-\beta^2-\ln I-\frac{\sum C_i}{Z}\right], \quad (1)$$

where dE/dx denotes the stopping power, e and m the charge and rest mass of the electron, z the atomic number of the incident particle, $\beta c=v$ the velocity of the incident particle, and N_0 Avogadro's number. Z, A, I, and $\sum C_i/Z$ indicate atomic number, atomic weight, mean ionization potential, and shell corrections of the target material, respectively.

The ionization potential I is an average over the excitation and ionization energies for the electrons in the target material. For the innermost electrons it is necessary to add corrections $\sum C_i/Z$, the shell corrections, which depend upon the velocity of the incoming particle. The index i denotes the different shells.

Walske[10,11] has calculated theoretically the K- and L-shell corrections for several elements. From these, Bichsel[6,7] calculated higher shell corrections by assuming that correction curves as a function of energy had the same shape as the L-shell correction curves. For each shell and for every element treated, he introduced two free parameters, scaling energy and magnitude of the corrections, respectively. The functions were fitted to a large number of the most reliable experimental range and stopping power data. The fits are claimed to be within 1% of the stopping power or within stated experimental errors.

II. EXPERIMENTAL PROCEDURE

The experimental method used in this experiment has been described in detail by Andersen,[12] and Andersen *et al.*[13]; thus, only the principle of the method will be given here.

A determination of the stopping power of metals for charged particles requires independent measurements of three quantities: energy loss in the metal foil, energy of the incoming particle, and thickness of the metal foil.

The principle for the measurement of the energy loss is shown in Fig. 1. The target foil and a metal block thicker than the range of the projectiles are connected to a liquid-helium reservoir through thermal resistances W_F and W_B. The beam passes through the foil and is stopped in the block. The energy lost by the particles causes a heating of foil and block giving temperature rises measured by the thermometers R_F and R_B. The

[1] H. Bichsel, W. Mozley, and W. A. Aron, Phys. Rev. **105**, 1788 (1957).
[2] H. Bichsel, Phys. Rev. **112**, 1089 (1958).
[3] L. P. Nielsen, Kgl. Danske Videnskab. Selskab, Mat.-Fys. Medd. **33**, No. 6 (1961).
[4] V. C. Burkig and K. R. MacKenzie, Phys. Rev. **106**, 848 (1957).
[5] G. H. Nakano, K. R. MacKenzie, and H. Bichsel, Phys. Rev. **132**, 291 (1963).
[6] H. Bichsel, Linear Accelerator Group, University of Southern California Technical Report No. TR-3, 1961 and 1963 (unpublished).
[7] H. Bichsel, *American Institute of Physics Handbook* (McGraw-Hill Book Company, Inc., New York, 1963), 2nd ed.
[8] H. Bichsel, Natl. Acad. Sci.—Natl. Res. Council Publ. 1133, 1964, p. 17.
[9] H. A. Bethe and J. Ashkin, in *Experimental Nuclear Physics*, edited by E. Segre (John Wiley & Sons, Inc., New York, 1953).
[10] M. C. Walske, Phys. Rev. **88**, 1283 (1952).
[11] M. C. Walske, Phys. Rev. **101**, 940 (1957).
[12] H. H. Andersen, Atomic Energy Commission, Denmark, Risö Report No. 93, 1965 (unpublished).
[13] H. H. Andersen, A. F. Garfinkel, C. C. Hanke, and H. Sørensen, Kgl. Danske Videnskab. Selskab, Mat.-Fys. Medd **35**, No. 4 (1966).

TABLE I. Thickness, thermal expansion correction, purity, and treatment of the applied foils.

Element	Approximate thickness mg/cm^{-2}	Thermal expansion correction %	Stated purity %	Treatment
Be	4.5 4.7 8.7	0.31	98.5(+1.2 BeO)	electroplated with Ag at soldering points, unannealed
Cu	9.9 18.5	0.68	99.9 99.999	annealed in vacuum at 550°C for 3–4 h
Ag	10.0 19.4	0.85	99.999	annealed in vacuum at 600°C for 4 h
Pt	10.4 19.2	0.40	99.999	annealed in vacuum at 800°C for 4 h
Au	9.3 18.5 18.9	0.76	99.999	annealed in air at 700–900°C for 3–7 h

beam is then switched off, and electric powers P_F and P_B are fed to heaters, thermally connected to foil and block, until the same temperature rises are obtained. A particle having energy E_0 immediately in front of the foil will suffer an energy loss ΔE in the foil given by the relation

$$\Delta E = E_0 \frac{P_F}{P_B + P_F}. \quad (2)$$

There are several advantages to be gained from this method. From (2) it is seen that ΔE is measured directly from the power ratio $P_F/(P_B+P_F)$. Conventional methods mostly measure the difference between initial and final particle energy. Furthermore, the beam need not to be focused on the target. In fact, the beam is spread out and limited by an aperture just in front of the target, so that ΔE is the mean energy loss over a certain area of the metal foil. Inhomogeneities in the foil thickness thus do not influence the results when the foil is irradiated uniformly.

There are several reasons for performing the experiments at liquid-helium temperature: (1) thermal radiation will be very small; (2) the absolute sensitivity of the thermometers is greater at lower temperatures, so that a smaller temperature rise is necessary to obtain a certain accuracy; (3) heat capacities are small and thermal conductivities high, resulting in small thermal time constants of the two systems.

The compensation technique may be erroneous either if there are radiation losses or if the heat dissipated by the beam does not choose the same heat paths to reach the reservoir as that supplied by the heaters. This has been investigated, and it was found that these sources of errors are negligible. We conclude that we measure the power ratio within 0.1%.

The foils were well annealed in the first measurements to ensure the highest possible heat conductivity. However, no trend in the power ratio was seen when unannealed foils were used. The annealing was then dispensed with as the unannealed foils were easier to handle.

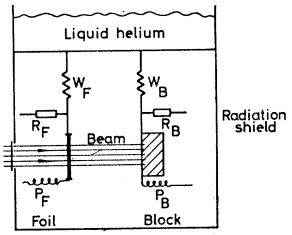

FIG. 1. Diagram of stopping power measuring system. W_F and W_B are thermal resistances, R_F and R_B thermometers, and P_F and P_B electrical heaters.

The measurements were done using the tandem Van de Graaff accelerator at the Niels Bohr Institute of the University of Copenhagen. To obtain E_0 with an accuracy comparable to that of the measured power ratio, the energies of the protons and deuterons coming from the analyzing magnet of the accelerator were calibrated using a heavy-particle spectrograph at another beam tube. The spectrograph, in its turn, is regularly calibrated with α particles of well-known energy. The mean energy E_0 is measured within 0.1% by this method. Because stopping power is roughly inversely proportional to energy in our energy range, and because E_0 is also used directly for calculation of dE/dx [see Eq. (2)], the uncertainty in E_0 contributes twice (0.2%) to the standard deviation of the tabulated stopping power values below.

After irradiation the irradiated part of the foil (6.5×13 mm) is cut out with a very accurately machined punching tool. The piece is weighed with a Cahn electrobalance, and the area is measured in a Leitz Ortholux microscope. This procedure was relatively easy for most of the irradiated foils. Only the thinnest gold foils were difficult to punch out. These were cut out with a razor blade. The error in the weight per area determination is estimated to be 0.1–0.15%.

During the measurements of ΔE, the foil is at liquid-helium temperature, while t, however, is measured at room temperature. A correction due to the thermal expansion of the foil material is applied. This correction will for some materials exceed 1%.

Table I gives for every element approximate foil thicknesses used, correction for thermal expansion, purities stated by manufacturers and treatment of the foils, if any, before measurements. Errors due to the stated maximum impurities in the beryllium foils and the most impure copper foil were calculated, and it was found that they did not exceed 0.1% in the worst cases.

III. TREATMENT OF EXPERIMENTAL DATA

When energy loss ΔE and foil thickness t are known, the stopping power S in a first-order approximation is

$$S(E') = \Delta E/t, \quad (3)$$

where $E' = E_0 - \Delta E/2$. Here E_0 denotes the energy of the particle immediately in front of the foil. A second-order correction has to be added to $S(E')$, as stopping power

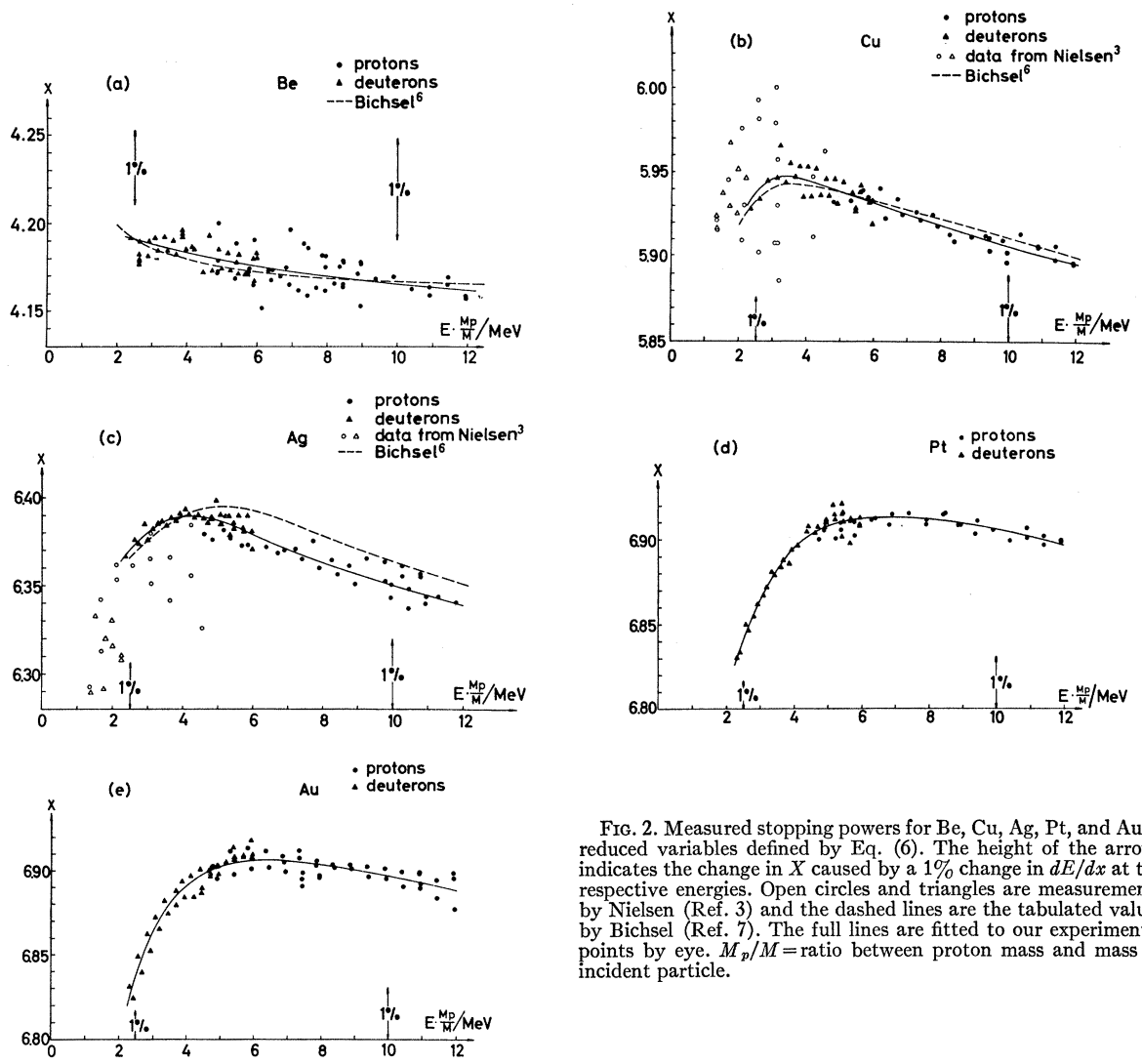

FIG. 2. Measured stopping powers for Be, Cu, Ag, Pt, and Au in reduced variables defined by Eq. (6). The height of the arrows indicates the change in X caused by a 1% change in dE/dx at the respective energies. Open circles and triangles are measurements by Nielsen (Ref. 3) and the dashed lines are the tabulated values by Bichsel (Ref. 7). The full lines are fitted to our experimental points by eye. M_p/M = ratio between proton mass and mass of incident particle.

changes while the particle traverses the foil. However, this correction turns out to be negligible for the foil thicknesses used here.

All particles suffer multiple scattering by the target nuclei when traversing the foil. This means that the average path length of a particle in the foil is greater than the foil thickness t. Also a small number of particles will be Coulomb-scattered through wide angles and lose nearly all their energy in the foil. Corrections for these effects are most important for low energies and for thick foils of heavy-element target materials, but totally they never exceed 0.5%.

A certain part of the energy given to the foil will escape through x rays. Auger effect and reabsorption have been taken into account by the calculation of the correction for this, which is largest for thin targets, high energies, and heavy elements ($\lesssim$0.4%).

High-energy secondary electrons (δ rays) emerging from the surface of the foil have also to be considered. For thin foils, heavy elements, and high energies the relative correction will have its maximum ($\simeq$0.5%). Detailed discussions of the corrections have been given previously.[12,13]

Corrections due to nuclear reactions in the foil, low-energy secondary electrons from the foil surface, sputtering of target atoms, stored energy due to radiation damage in the foil and the block, and crystallographic effects like channeling are found to be negligible.

IV. RESULTS AND DISCUSSION

The energy variation of the stopping power is mainly given by $\ln E/E$ [Eq. (1)]. This term varies so rapidly with energy that it is impossible to see small deviations from this energy dependence, when the stopping power is plotted directly. We have therefore used Bichsel's X function,[8] which is defined in the following way

TABLE II. Smoothed values of measured stopping powers for protons in Be, Cu, Ag, Pt, and Au obtained from the full lines in Fig. 2. Al from Ref. 13. Experimental standard error ±0.3%.

Energy (MeV)	Stopping power $-dE/dx$ (keV/mg cm^{-2}) Be	Al	Cu	Ag	Pt	Au
2.25	122.70	101.92	75.19	59.63	42.85	43.12
2.50	113.21	94.68	70.28	56.18	40.67	40.87
2.75	105.19	88.52	66.07	53.16	38.71	38.89
3.00	98.36	83.19	62.44	50.46	36.97	37.11
3.25	92.42	78.56	59.25	48.07	35.39	35.52
3.50	87.24	74.51	56.43	45.94	33.96	34.09
3.75	82.65	70.94	53.91	44.02	32.66	32.79
4.00	78.57	67.76	51.65	42.28	31.47	31.62
4.25	74.90	64.85	49.60	40.70	30.39	30.55
4.50	71.60	62.21	47.72	39.26	29.40	29.56
4.75	68.58	59.80	45.99	37.93	28.49	28.65
5.00	65.87	57.59	44.42	36.71	27.65	27.79
5.25	63.36	55.56	42.95	35.58	26.85	27.00
5.50	61.06	53.68	41.59	34.53	26.12	26.25
5.75	58.93	51.93	40.33	33.55	25.43	25.56
6.00	56.96	50.31	39.15	32.63	24.79	24.91
6.50	53.42	47.38	37.01	30.97	23.60	23.72
7.00	50.34	44.81	35.12	29.48	22.54	22.67
7.50	47.62	42.52	33.44	28.14	21.58	21.73
8.00	45.21	40.47	31.93	26.94	20.72	20.85
8.50	43.05	38.64	30.57	25.85	19.94	20.06
9.00	41.10	36.97	29.33	24.86	19.22	19.34
9.50	39.34	35.46	28.21	23.95	18.56	18.67
10.00	37.74	34.08	27.17	23.11	17.95	18.06
10.50	36.27	32.82	26.22	22.34	17.39	17.49
11.00	34.93	31.66	25.35	21.62	16.88	16.97
11.50	33.69	30.58	24.54	20.96	16.39	16.48
12.00	32.54	29.58	23.78	20.34	15.93	16.02
Atomic weight	9.013	26.98	63.54	107.88	195.09	197.00

[cf. Eq. (1)]:

$$S=(Z/A)K(\beta)[f(\beta)-X], \tag{4}$$

where

$$S=-dE/dx,$$

$$K(\beta)=\frac{4\pi e^4z^2}{mc^2\beta^2}N_0,$$

$$f(\beta)=\ln\left(\frac{2mc^2\beta^2}{1-\beta^2}\right)-\beta^2,$$

$$X=\ln I+(\sum C_i)/Z. \tag{5}$$

$K(\beta)$ and $f(\beta)$ can be calculated, and experimental values of X are expressed explicitly by

$$X_{\text{exp}}=f(\beta)-\frac{AS_{\text{exp}}}{ZK(\beta)}. \tag{6}$$

Inserting for $S(E)$ the experimental values, we get for each element a set of points to which a smooth curve is fitted by eye (Fig. 2). Deuteron points are plotted at the energy EM_p/M_d, where M_p and M_d are the masses of proton and deuteron, respectively, (M_p=938.214 MeV, M_d=1875.5 MeV) because particles with the same velocity should have the same stopping power [cf. Eq. (1)]. From (6) it is seen that numerically X decreases with increasing stopping power. The 1% arrows indicate the change in X, caused by a 1% change in stopping power at the respective energy. Table II gives the stopping powers for protons of Be, Al, Cu, Ag, Pt, and Au in keV/mg cm^{-2} from 2.25 to 12.0 MeV. The deuteron-stopping powers are thus reduced to proton-stopping powers at the energy EM_p/M_d. The numbers in the Table were found by taking X values from the fitted curves and calculating the corresponding $S(E)$ using Eq. (6). The aluminum data are taken from Ref. 13. Combination of the errors listed in the preceding paragraphs yields a total standard deviation in the tabulated values of 0.3%, including the uncertainties in the applied corrections. Table II also includes the atomic weights of the materials used in the calculation of X.

TABLE III. Present stopping powers for 12-MeV protons relative to aluminum compared to results by Teasdale (Ref. 15).

Element	(A) Teasdale	(B) Present data	(A−B)/A
Cu	0.810±0.6%	0.804±0.4%	+0.8%
Ag	0.698±1.0%	0.688±0.4%	+1.5%
Ag	0.692±0.9%	0.688±0.4%	+0.6%
Pt	0.549±0.7%	0.539±0.4%	+1.9%
Au	0.553±1.1%	0.542±0.4%	+2.1%
Au	0.543±0.9%	0.542±0.4%	+0.3%

The absolute stopping power measurements by Nielsen[3] are shown as open circles and triangles in Fig. 2. For beryllium and gold some of her points could not be contained within our figures, and for these elements we have not plotted any of her data. However, the results agree within her stated errors.

A recent measurement of absolute energy loss of 28-MeV alpha particles in gold by Hosono *et al.*[14] gives the value 89.2±1.5 keV/mg cm^{-2} (at 28.12 MeV, equivalent to a proton energy of 7.08 MeV). Interpolation from our table gives 22.52±0.07 keV/mg cm^{-2} for protons, which is multiplied by 4 because of the double charge of the alpha particle giving 90.1±0.3 keV/mg cm^{-2}. Our value is about 1% higher than that by Hosono *et al.*, but the agreement is within the stated error.

Table III shows a comparison of our experiments with the stopping power measurements of several elements relative to aluminum for 12-MeV protons by Teasdale.[15] The present data are systematically lower, but they all agree within the claimed standard deviations.

The dashed lines in Fig. 2 indicate the stopping powers tabulated by Bichsel.[7] They are claimed to be accurate to 1%, and from the figure it is seen that our data agree within this error.

The extensive tables of Barkas and Berger[16] fit our results only to about 2%. The X values computed from their tables show such large fluctuations that they could not be contained in the figures.

[14] K. Hosono, R. Ishiwari, Y. Uemura, Bull. Inst. Chem. Res. (Kyoto) 43, 323 (1965).

[15] John G. Teasdale, University of California at Los Angeles, Report No. NP-1368, 1949 (unpublished).

[16] W. H. Barkas and M. J. Berger, Natl. Acad. Sci.–Natl. Res. Council Publ. 1133, 1964, p. 103.

The work described here is continued with other elements, and measurements on a series of neighboring elements ($Z=22$–30) are in progress. From the results we hope to get more detailed information about the influence of the shell structure.

ACKNOWLEDGMENTS

Thanks are due to the Niels Bohr Institute, the University of Copenhagen, for letting us use the tandem Van de Graaff accelerator. HHA thanks the Technical University of Copenhagen for a fellowship, and PV thanks the International Atomic Energy Agency for a fellowship during part of the time. We appreciate the valuable assistance of B. Bordrup, G. Dalsgaard, and A. Nordskov Nielsen in the experimental part of the work. With Professor H. Bichsel we have had a prolific correspondence, and great stimulation came from the interest of Professor O. Kofoed-Hansen and Professor J. Lindhard.

PHYSICAL REVIEW VOLUME 153, NUMBER 2 10 JANUARY 1967

Some Features of the Nonlinear Optical Field

P. A. SILBERG*
Advanced Development Laboratory, Raytheon Company, Wayland, Massachusetts
(Received 8 September 1965; revised manuscript received 26 May 1966)

In a recent paper, Chiao, Garmire, and Townes (CGT) discuss self-trapping of optical beams by a nonlinear dielectric. This work has been extended in the present paper by showing that the nonlinear wave equation, written in Cartesian coordinates, has, under certain restrictions, a solution in terms of Jacobian elliptic functions. This solution transforms smoothly into the sine and cosine functions as the nonlinear term vanishes, and in accordance with the CGT solution. Moreover, the tabulated properties of the elliptic functions predict other properties of the nonlinear optical field which could be checked with several experiments.

INTRODUCTION

IN a recent paper, Chiao, Garmire and Townes (CGT)[1] discuss the self-trapping of optical beams by a nonlinear dielectric mechanism for which the dielectric constant is expressed as[2]

$$\epsilon=\epsilon_0+\epsilon_2E^2, \tag{1}$$

and the index of refraction

$$n=n_0+n_2E^2+\cdots. \tag{2}$$

The mechanism which is then proposed for self-trapping of optical beams is obtained by considering the diffraction of a circular optical beam of uniform intensity in the nonlinear dielectric. It is pointed out that under linear conditions, the beam might be expected to expand or diverge owing to diffraction, but if the nonlinearity of the dielectric is also considered, then the term n_2E^2 under suitable circumstances can produce an index of refraction within the beam which is so high that the critical angle for total internal reflection at the beam's boundary is greater than the diffraction angle, so that no beam spreading by diffraction can occur. The arguments used for the most part are simple and straightforward. The wave equation containing the nonlinear term is solved for several special cases. The implications of the work of CGT suggest a greater exploration of the nonlinear mechanism. Consequently, the purpose of the present paper is to extend the work of CGT and to more fully examine the nonlinear mechanism.

We begin with the nonlinear Eq. (3) of CGT and seek a three-dimensional solution in the Cartesian-coordinate system. This solution turns out to be a Jacobi elliptic function, whose properties are then examined relative to wave propagation. Two experiments are suggested to check the predictions of the analysis.

DISCUSSION

We will begin by writing Eq. (3) of CGT as

$$\nabla^2\mathbf{E}-\frac{\epsilon_0}{c^2}\frac{\partial^2}{\partial t^2}\mathbf{E}-\frac{\epsilon_2}{c^2}\frac{\partial^2}{\partial t^2}(E^2\mathbf{E})=0, \tag{3}$$

and assume with CGT that a relaxation mechanism is present within the dielectric. In this connection it is worth pointing out that one important relaxation mechanism is the resonance effects of electrons, ions, and atoms in the optical spectral region.[2] Other relaxation mechanisms specifically mentioned by CGT are the electrostrictive effects and the electro-optical Kerr effect, which in general are slower than the optical oscillation. The relaxation assumption requires that a complex dielectric constant be used.[2]

$$\epsilon^*=\epsilon(\cos\delta-j\sin\delta)=\epsilon'-j\epsilon'', \tag{4}$$

* Now at Northrop Corp., Norwood, Mass.
[1] R. Y. Chiao, E. Garmire, and C. H. Townes, Phys. Rev. Letters 13, 479 (1964), hereafter referred to as CGT.
[2] C. J. Bottcher, *The Theory of Electric Polarization* (Elsevier Publishing Company, New York, 1952), p. 228.